

Modeling Proton-Bound Methanol, Ammonia, and Amine Complexes of 12-Crown-4-Ether and Dimethoxyethane (“Glyme”) Using Density Functional Theory

Dora Adötoledo,[†] Viktoriya Aviyente,[†] Jan M. L. Martin,^{‡,||} and Chava Lifshitz^{*,§,⊥}

Chemistry Department, Bogaziçi University, 80815, Bebek, Istanbul, Turkey, Department of Organic Chemistry, Weizmann Institute of Science, Rehovot 76100, Israel, and Department of Physical Chemistry and the Farkas Center for Light Induced Processes, The Hebrew University of Jerusalem, 91904, Jerusalem, Israel

Received: April 2, 1998; In Final Form: May 11, 1998

The association reactions undergone by 12-crown-4-ether, 12c4H⁺, with NH₃, CH₃OH, CH₃NH₂, (CH₃)₂NH, and (CH₃)₃N have been studied using the B3LYP density functional method and a variety of basis sets. For comparison purposes the insertion reactions for the same bases into protonated dimethoxyethane (“glyme”), GI·H⁺, and protonated glyme dimer, (GI)₂H⁺, have also been modeled. The B3LYP/aug-cc-pVDZ//B3LYP/4-21G(*) level of theory was found to be a particularly favorable compromise between accuracy and computational expense for the calculation of proton affinities of medium-sized species. The protonated glyme, GI·H⁺, the protonated glyme dimer, (GI)₂H⁺, and the protonated crown ether, 12c4H⁺, form two internal hydrogen bonds with NH₃, CH₃OH, CH₃NH₂, and (CH₃)₂NH, except for (GI)₂H⁺·NH₃ which has four O···H bonds. In GI·NH(CH₃)₃⁺, there is a single O···H bond and the protons of the methyl groups assist weakly in O···HC bonding. The insertion energy of methanol, ammonia, and the series of amines into 12c4H⁺ increases with increasing proton affinity of the inserting base. A similar trend is observed for insertion into (GI)₂H⁺. Trimethylamine does not follow the expected trend because it forms proton-bound complexes that have a single O···HN bond instead of two. The association energy of CH₃OH₂⁺, NH₄⁺, etc., with 12c4 or GI₂ decreases with increasing proton affinity (of methanol, ammonia, etc.).

I. Introduction

Crown ethers have been of great interest since their first synthesis by Pedersen in 1967.¹ The ability of polyethers—glymes, crown ethers, and cryptands—to act as very effective complexing agents for cations is well established and represents a field of great chemical and biological significance.²

The importance of determining thermochemical properties for complexation of cations by polyethers, in the absence of solvent and counterions, has been pointed out.^{2b,3,4} Alkali metal—crown ether complexes have been studied by collision-induced dissociation threshold energy determinations employing guided ion beam experiments,^{2b} while the specific species under study here have been studied using pulsed high-pressure mass spectrometry by Meot-Ner³ and by Kebarle and co-workers.⁴

The thermochemistry of internal hydrogen bonds and of multiple hydrogen bonding was estimated by comparisons between polyfunctional and analogous monofunctional ions.³ Polyethers, crown ethers, and glymes exhibit strong (30 kcal/mol) internal hydrogen bonds, stabilizing the protonated species and increasing the PAs of the corresponding molecules.^{5,6} The hydrogen bonding of polyfunctional molecules with polyprotonic ions leads to multiply hydrogen bonded structures, which leads to stabilization of ion/molecule complexes;⁵ this was observed for ammonia—crown ether³ and methoxonium (CH₃OH₂⁺)—crown ether complexes.⁴

Reactions of protonated 12-crown-4 ether (12c4H⁺) and its ammonium and methoxonium ion complexes with a series of base molecules were studied using a selected ion flow tube.⁷ Reaction efficiencies were observed to be enhanced for base molecules capable of forming multiple hydrogen bonded structures. The association reactions undergone by 12c4H⁺ with ammonia and methanol were viewed⁷ as insertion reactions analogous to reactions observed for alkyl-blocked dimers such as (CH₃CN)₂H⁺.^{8–10}

In previous work,¹¹ we have modeled the insertion reactions of ammonia, methylamine, dimethylamine, and methanol into proton-bound alkyl-blocked dimers of acetonitrile, (CH₃CN)₂H⁺, and acetone, (CH₃COCH₃)₂H⁺, using hybrid density functional methods and have explained their insertion mechanism. The purpose of the present work is to shed light on the reactions of bases with protonated glyme GI·H⁺, protonated glyme dimer-(GI)₂H⁺, and proton-bound 12-crown-4-ether (12c4H⁺), with the same computational method.

II. Methods

All density functional calculations have been carried out using the Gaussian 94 package¹² running on a DEC Alpha TurboLaser 8400 at the Institute of Chemistry, Hebrew University; on a DEC Alpha 233/4 at the Chemistry Department, Bogaziçi University, and on DEC Alpha 500/500 and Silicon Graphics Origin 2000 computers at the Weizmann Institute of Science. Semiempirical calculations using the PM3 model¹³ were performed using Spartan.¹⁴

All density functional calculations employed the B3LYP (Becke three-parameter-Lee–Yang–Parr) exchange–correlation functional,^{15,16} which combines the Becke three-parameter

[†] Bogaziçi University.

[‡] Weizmann Institute of Science.

[§] The Hebrew University of Jerusalem.

^{||} Incumbent of the Helen and Milton A. Kimmelman Career Development Chair.

[⊥] Archie and Marjorie Sherman Professor of Chemistry.

TABLE 1: B3LYP Computed Dissociation Enthalpies at 298 K (kcal/mol) for the Different Complexes

reaction	4-21G(*)	VDZ//4-21G(*)	AVDZ//4-21G(*)
GIH ⁺ (12) → GI(11) + H ⁺ (I)	222.57	207.35	203.63
GI·CH ₃ OH ₂ ⁺ (13) → GIH ⁺ (12) + CH ₃ OH (II)	35.61	26.34	20.92
GI·CH ₃ OH ₂ ⁺ (13) → GI(11) + CH ₃ OH ₂ ⁺ (III)	64.35	49.54	45.44
GI·NH ₄ ⁺ (14) → GIH ⁺ (12) + NH ₃ (IV)	43.72	38.77	33.27
GI·NH ₄ ⁺ (14) → GI(11) + NH ₄ ⁺ (V)	48.24	37.40	34.66
GI·NH ₃ CH ₃ ⁺ (15) → GIH ⁺ (12) + NH ₂ CH ₃ (VI)	46.56	44.15	40.21
GI·NH ₃ CH ₃ ⁺ (15) → GI(11) + NH ₃ CH ₃ ⁺ (VII)	45.99	33.18	29.97
GI·NH ₂ (CH ₃) ₂ ⁺ (16) → GIH ⁺ (12) + NH(CH ₃) ₂ (VIII)	49.14	46.89	44.34
GI·NH ₂ (CH ₃) ₂ ⁺ (16) → GI(11) + NH ₂ (CH ₃) ₂ ⁺ (IX)	40.07	30.30	26.94
GI·NH(CH ₃) ₃ ⁺ (17) → GIH ⁺ (12) + N(CH ₃) ₃ (X)	46.88	43.59	42.10
GI·NH(CH ₃) ₃ ⁺ (17) → GI(11) + NH(CH ₃) ₃ ⁺ (XI)	33.33	23.96	20.48
(GI) ₂ H ⁺ (18) → 2GI(11) + H ⁺ (XII)	256.67	234.23	226.98
(GI) ₂ H ⁺ (18) → GI(11) + GIH ⁺ (12) (XIII)	34.10	26.88	23.35
(GI) ₂ CH ₃ OH ₂ ⁺ (19) → (GI) ₂ H ⁺ (18) + CH ₃ OH (XIV)	26.05	19.11	13.71
(GI) ₂ CH ₃ OH ₂ ⁺ (19) → 2(GI) + CH ₃ OH ₂ ⁺ (XV)	88.89	69.19	61.58
(GI) ₂ NH ₄ ⁺ (20) → (GI) ₂ H ⁺ (18) + NH ₃ (XVI)	45.77	34.83	30.59
(GI) ₂ NH ₄ ⁺ (20) → 2(GI) + NH ₄ ⁺ (XVII)	84.39	60.34	55.33
12c4H ⁺ (22) → 12c4(21) + H ⁺ (XVIII)	231.07	218.55	216.94
12c4H ⁺ ·CH ₃ OH(23) → 12c4H ⁺ (22) + CH ₃ OH (XIX)	35.79	27.18	20.04
12c4H ⁺ ·CH ₃ OH(23) → 12c4(21) + CH ₃ OH ₂ ⁺ (XX)	73.02	61.58	57.87
12c4H ⁺ ·NH ₃ (24) → 12c4H ⁺ (22) + NH ₃ (XXI)	45.67	39.62	33.13
12c4H ⁺ ·NH ₃ (24) → 12c4(21) + NH ₄ ⁺ (XXII)	58.69	49.44	47.82
12c4H ⁺ ·NH ₂ CH ₃ (25) → 12c4H ⁺ (22) + NH ₂ CH ₃ (XXIII)	49.55	44.65	38.96
12c4H ⁺ ·NH ₂ CH ₃ (25) → 12c4(21) + NH ₃ CH ₃ ⁺ (XXIV)	57.48	44.87	42.03
12c4H ⁺ ·NH(CH ₃) ₂ (26) → 12c4H ⁺ (22) + NH(CH ₃) ₂ (XXV)	50.89	45.64	41.09
12c4H ⁺ ·NH(CH ₃) ₂ (26) → 12c4(21) + NH ₂ (CH ₃) ₂ ⁺ (XXVI)	50.32	40.24	37.01
12c4H ⁺ ·N(CH ₃) ₃ (27) → 12c4H ⁺ (22) + N(CH ₃) ₃ (XXVII)	41.88	38.36	35.21
12c4H ⁺ ·N(CH ₃) ₃ (27) → 12c4(21) + N(CH ₃) ₃ H ⁺ (XXVIII)	36.83	29.93	26.89

hybrid exchange functional¹⁵ with the gradient-corrected correlation functional of Lee, Yang, and Parr.¹⁶ The excellent performance of this method has been noted previously for geometries and harmonic frequencies.¹⁷

Geometry optimizations and harmonic frequency calculations were carried out using the 4-21G(*) basis set, which stands for the standard 4-21G basis set of Pulay et al.¹⁸ with a single d polarization function added on all heteroatoms as well as on hydrogen atoms involved in protonation and/or hydrogen bonding. (An early example of the use of such mixed basis sets in geometry optimizations can be found in the work of Pang et al.¹⁹ on the structure of some nitrogen heteroaromatics.) The exponents for these extra functions were taken from Dunning's cc-pVDZ (correlation consistent polarized valence double- ζ) basis set.^{20a}

Using the B3LYP/4-21G(*) reference geometries, single-point calculations of the energetics were carried out at the B3LYP level with the following larger basis sets: (a) cc-pVDZ, which is of [3s2p1d/2s1p] quality; (b) the larger cc-pVTZ (correlation consistent polarized valence triple- ζ) basis set, which is of [4s3p2d1f/3s2p1d] quality; (c, d) the aug-cc-pVDZ and aug-cc-pVTZ (augmented correlation consistent polarized valence double- and triple- ζ , respectively) basis sets of Kendall et al.,^{20b} which differ from the parent cc-pVnZ basis sets by the addition of one low-exponent ("diffuse") function of each angular momentum present. The latter were developed with improved performance for electron affinities in mind, but the diffuse functions were previously (e.g., ref 21) found to be essential in obtaining high-accuracy proton affinities as well (because protonation generally involves a change in the number of free electron pairs). The aug-cc-pVDZ and aug-cc-pVTZ basis sets (AVDZ and AVTZ for short) are of [4s3p2d/3s2p] and [5s4p3d2f/4s3p2d] quality, respectively.

In addition, we considered improvement of the B3LYP/4-21G(*) energetics with a BSSE (basis set superposition error) correction according to the Boys–Bernardi counterpoise method.²³

Zero-point energies and RRHO (rigid rotor-harmonic oscillator) thermal corrections at 298 K were computed from the

unscaled B3LYP/4-21G(*) harmonic frequencies. The latter were also essential to verify that some of the structures obtained for the floppier molecules were in fact local minima.

Total energies and zero-point energies are given as Supporting Information. Binding energies, i.e., differences in energy between the dissociation products and the reactant, including the zero-point energies are given in Table 1. Table 2 presents calculated and experimental thermochemical data. The procedure used by Yamabe et al.²² was followed to calculate proton affinities as

$$-PA = \Delta E + \Delta E_{\text{vib}} + \text{BSSE} + (-5/2)RT \quad (1)$$

$(-5/2)RT$ is the thermal correction of translation and rotation. For the B3LYP/4-21G(*) thermochemical data, estimated BSSE corrections according to the Boys–Bernardi counterpoise method²³ were also considered.

Atomic polarizability tensor (APT) population analysis^{24a} was carried out for these structures using the program GAR2PED^{24b} as in our previous work.¹¹ For a recent comparative study of the performance of DFT methods for different charge distributions, see ref 24c.

The geometries for the structures that were characterized as local minima are given in Figures 1–4, together with APT charges for the atoms directly involved in protonation.

III. Results and Discussion

1. Proton Affinities of the Smaller Species. Comparison of computed B3LYP/4-21G(*) PAs with experiment for these species reveals that the calculated values leave a lot to be desired. BSSE corrections are found to be very sizable, reaching 15.7 kcal/mol for GI₂H⁺ and 8.1 kcal/mol for CH₃OH. After BSSE correction, the values are still systematically too high. Moreover, the calculated–observed gap is anything but constant or systematic, strongly suggesting that the B3LYP/4-21G(*) level of theory, even with counterpoise correction, is simply inadequate.

TABLE 2: Comparison of Calculated and Observed Reaction Enthalpies (kcal/mol) at 298 K. Estimates of BSSE by the Counterpoise Method, Where Available, Are Given in Parentheses

reaction	B3LYP/4-21G(*)	B3LYP/VDZ	B3LYP/VTZ	B3LYP/AVDZ	B3LYP/AVTZ	experiment
$\text{CH}_3\text{OH}_2^+ \rightarrow \text{CH}_3\text{OH} + \text{H}^+$	193.84 (8.1)	184.16 (3.75)	182.25 (1.20)	179.11 (0.25)	180.32 (0.08)	181.9 ^c
$\text{NH}_4^+ \rightarrow \text{NH}_3 + \text{H}^+$	218.06 (5.4)	208.72 (3.96)	205.78 (1.49)	202.24 (0.47)	203.39 (0.07)	204 ^c , 203.5 ^d
$\text{NH}_3\text{CH}_3^+ \rightarrow \text{NH}_2\text{CH}_3 + \text{H}^+$	226.85 (5.2)	218.32 (2.13)	216.56 (0.85)	213.86 (0.62)	214.86 (0.07)	214.1 ^c , 215.4 ^d
$\text{NH}_2(\text{CH}_3)_2^+ \rightarrow \text{NH}(\text{CH}_3)_2 + \text{H}^+$	231.66 (3.5)	223.96 (3.05)	223.16 (1.13)	221.04 (0.40)	221.97 (0.14)	220.6 ^c , 222.5 ^d
$\text{N}(\text{CH}_3)_3\text{H}^+ \rightarrow \text{N}(\text{CH}_3)_3 + \text{H}^+$	236.14 (4.5)	227.00 (2.46)	226.98 (0.92)	225.28 (0.46)	226.12 (0.16)	225.1 ^c
$\text{GIH}^+ \rightarrow \text{GI} + \text{H}^+$	222.58 (8.7)	207.36 (2.56)	205.73 (0.58)	203.64 (0.33)	[204.7] ^s	204.9 ^c , 208.9 ^e
$(\text{GI})_2\text{H}^+ \rightarrow 2\text{GI} + \text{H}^+$	256.66 (16.8)	234.2		227.0	[227.9] ^s	236 ^c
$12\text{c}4\text{H}^+ \rightarrow 12\text{c}4 + \text{H}^+$	231.08 (8.4)	218.6	218.3	217.0	[217.9] ^s	219.6 ^a , 221.0 ^b , 225.0 ^c
$12\text{c}4\text{H}^+\cdot\text{CH}_3\text{OH} \rightarrow 12\text{c}4\text{H}^+ + \text{CH}_3\text{OH}$	35.78 (11.6)	27.2		20.0		19.5 ^f
$12\text{c}4\text{H}^+\cdot\text{CH}_3\text{OH} \rightarrow 12\text{c}4 + \text{CH}_3\text{OH}_2^+$	73.02 (18.4)	61.6		57.9		58.3 ^f

^a Ref 6. ^b Ref 36. ^c Ref 37. ^d Ref 35. ^e Ref 28. ^f Ref 10. ^s Extrapolated values using eq 2.

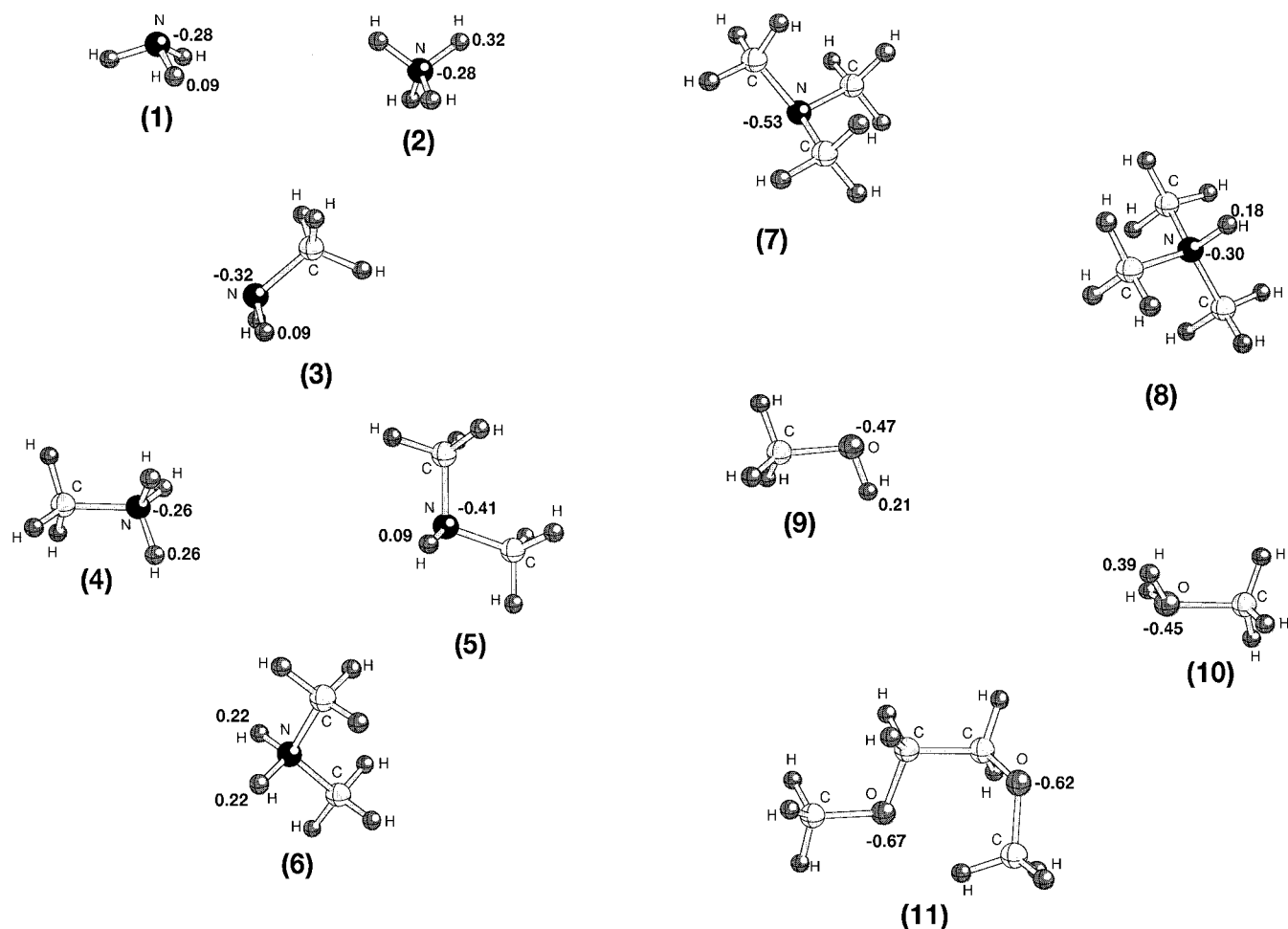


Figure 1. B3LYP/4-21G(*) computed structures of the species 1–11 as well as hydrogen bond distances (Å) and APT atomic charges of some relevant atoms.

Using a cc-pVDZ basis set instead appears to improve results somewhat. The calculated–observed difference now however displays a clear trend of increasing with increasing basicity. Switching to the AVDZ basis set remedies this problem: all computed PAs are now systematically slightly too low. Our explanation is that with increasing PA and thus increasing

“anionlike” character of the proton acceptor atom in the neutral species diffuse functions afford an increasingly larger stabilization to the neutral. Hence their absence would result in a progressively larger artificial increase of the PA (because the basis set is progressively more biased against the neutral) with increasing basicity, as observed.

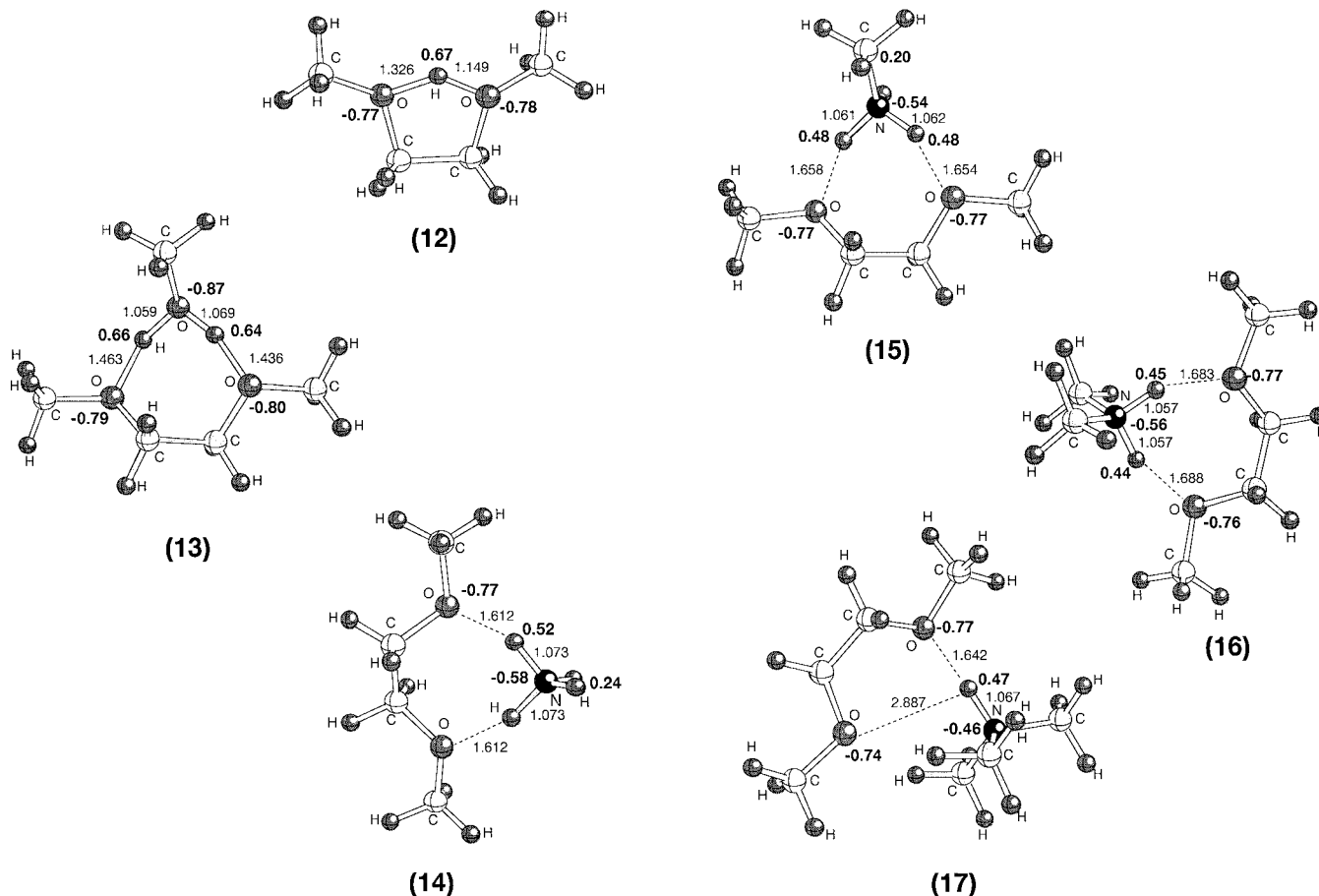


Figure 2. B3LYP/4-21G(*) computed structures of the species 12–17 as well as hydrogen bond distances (Å) and APT atomic charges of some relevant atoms.

As expected, the VTZ results are significantly better than the VDZ results, but still exhibit a greater-than-unity slope for a regression of computed versus observed values. The effect is however much milder because the outermost primitives of the cc-pVTZ basis set are considerably more “diffuse” than those in the cc-pVDZ basis set. As expected, this tendency disappears upon switching to the AVTZ basis set, the B3LYP/AVTZ values being consistently close to the experimental ones. The difference between B3LYP/AVDZ and B3LYP/AVTZ values is however quite small and definitely out of all proportion with the great increase in computational expense involved. (The AVDZ basis set involves 20 basis functions per first-row atom and 9 per hydrogen, compared to 46 and 20, respectively, for AVTZ.) Moreover, for the five proton affinities we have here, a linear regression (in kcal/mol)

$$\text{PA}[\text{AVTZ}] = 0.9922(16)\text{PA}[\text{AVDZ}] + 2.64(34) \quad (2)$$

has a correlation coefficient $R = 0.99999$ and residuals of 0.08 kcal/mol or less. Hence we propose to simply use this equation to somewhat further improve on the computed B3LYP/AVDZ results for the bigger species.

A critical reader would rightly argue that the excellent agreement with experiment at the B3LYP/AVDZ and particularly B3LYP/AVTZ level might be a result of error compensation involving neglect of BSSE. To address this point, we have computed counterpoise (CP) corrections using the larger basis sets, wherever our computational resources permitted us doing so. (These corrections can likewise be found in Table 2.) We see here that the CP corrections are smaller with the cc-pVDZ

than with the 4-21G(*) basis set; the most conspicuous feature, however, is that adding on diffuse functions to obtain the AVDZ basis set reduces the estimated BSSE by almost an order of magnitude. Indeed, ranging from 0.25 to 0.62 kcal/mol for the systems surveyed, they are appreciably smaller than those with the *larger* cc-pVTZ basis set (0.58–1.49 kcal/mol); those with the AVTZ basis set, at 0.07–0.16 kcal/mol, can definitely be called negligible in the context of the present work. In other words, the improvement in agreement with experiment is clearly paralleled by a strong reduction in the estimated BSSE.

A similar phenomenon was observed in a recent *ab initio* convergence study^{23b} on the water dimer interaction energy, where adding diffuse functions to a [5s4p3d2f1g/4s3p2d1f] basis set was found to reduce the CP correction to it by an order of magnitude at the SCF level and still by a factor of 4 at the CCSD(T) coupled cluster level. Likewise, in a recent calibration study^{23c} on the anharmonic force field of acetylene, an unphysical anharmonicity and grossly underestimated harmonic frequency with basis sets as large as [5s4p3d2f1g/4s3p2d1f] were found to disappear completely upon adding diffuse functions to the basis set: exploratory calculations led to a tentative diagnosis of the problem as dynamical BSSE.

2. Glyme and Related Complexes. The structure of dimethoxyethane (DME, dimethyl glycol ether, “glyme”), G1 (11), has been investigated extensively theoretically and experimentally in the past decade.^{25a–d,26a–h} Analyses of infrared and Raman spectra showed that the CH₂–CH₂ bond is *gauche* in the crystal mixture,^{25a} and the *ttt* (trans-trans-trans) and *tgt* (trans-gauche-trans) rotamers were found in the liquid and gas phases.^{25b–e} Astrup reported from electron diffraction measure-

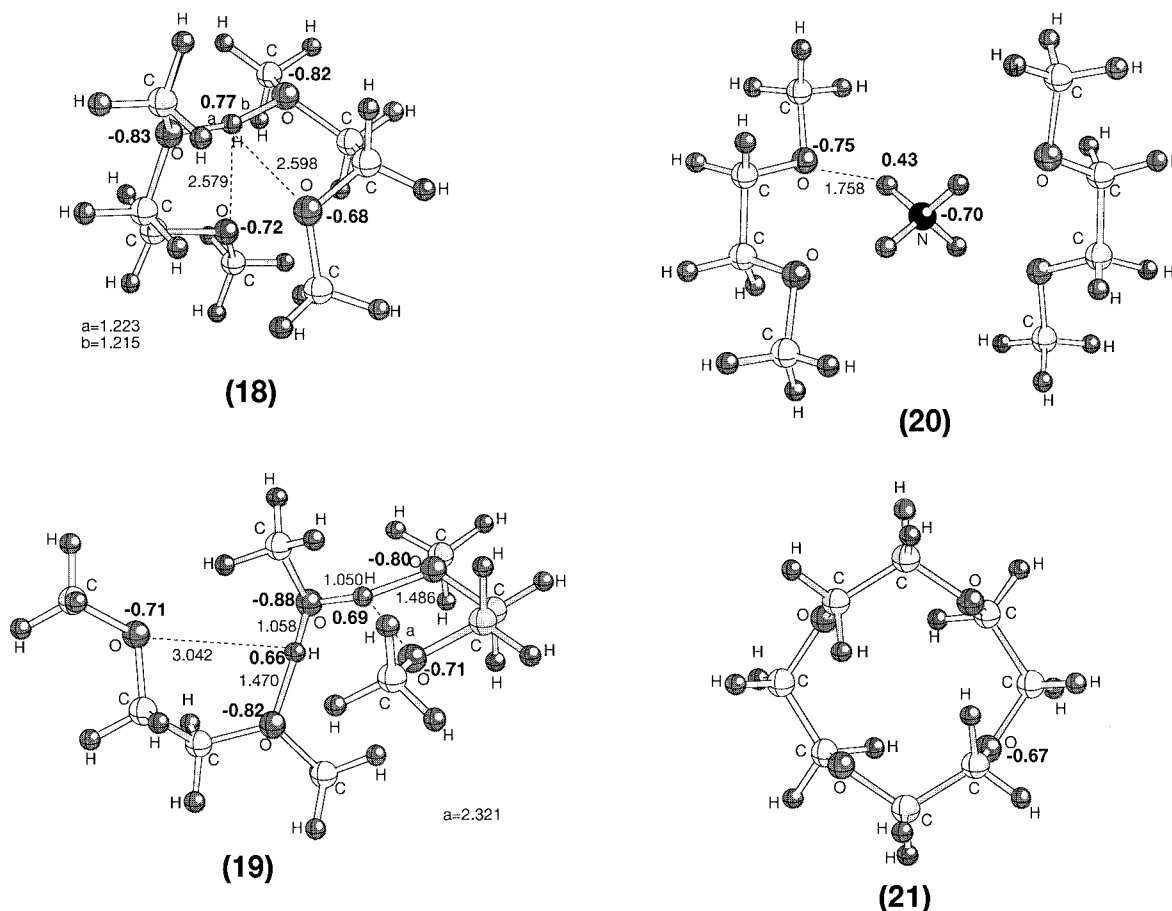


Figure 3. B3LYP/4-21G(*) computed structures of the species **18**–**21** as well as hydrogen bond distances (Å) and APT atomic charges of some relevant atoms.

ments that several rotamers exist in the gas phase.^{26f} Jaffe et al.^{26g} investigated the dependence of the conformational energies of the 10 unique rotamers of DME on the basis set and the level of electron correlation treatment. They found the *ttt* conformer (which has C_{2h} symmetry) to be the global minimum and *tgt* (which has C_2 symmetry) to be the next lowest conformer. However, introduction of electron correlation strongly reduces the conformational energy difference $\Delta E_{ttt,tgt}$, as does improving the basis set at the correlated level, resulting in a $\Delta E_{ttt,tgt}$ of only 0.10 kcal/mol as their best estimate. Feller and co-workers,^{26h} using geometric basis set extrapolation techniques^{26k} in conjunction with basis sets of up to spdfg quality, found a similarly small value as their best estimate.

The tg^+g^- conformer (C_1 symmetry) was found by Jaffe et al. to be the third lowest in energy ($\Delta E = 0.23$ kcal/mol, agreeing to within 0.1 kcal/mol with recent measurements^{26l}). Since it however is 4-fold “degenerate” in rotamer space, it was predicted by them to have the highest relative abundance at 0 °C, followed by *tgt* (which is 2-fold “degenerate”) and *ttt* (which is not “degenerate”): their computed rotamer populations were in very good agreement with those obtained by Astrup^{26f} from electron diffraction experiments.^{26f} (For comparison, recently Brickmann et al.^{26j} have shown that for 1,2-ethanediol (glycol), at the MP2 level using basis sets up to 6-311+G(3df,3pd), the conformations where the oxygen atoms are gauche to each other are preferred over the others by at least 2 kcal/mol.) Abe²⁷ has claimed that the gauche preference for the OC–CO bond is not a feature caused by the surrounding solvent molecules in solution.

In this work, a rotamer search around the five single bonds was first performed with the PM3 semiempirical method. This method is clearly not sufficient, yielding *ttt* as the *least* favorable structure and $tg^+g^- < tgt < g^+tg^-$ as the lowest three conformers. (Jaffe et al. found g^+tg^- as the fourth highest rotamer.) At the B3LYP/4-21G(*) level, this ordering changes to $tg^+g^- < ttt < tgt < g^+tg^-$: improving the basis set to cc-pVDZ brings the bottom three conformers much closer to each other and strongly increases the separation from the g^+tg^- rotamer. Further improving the basis set to AVDZ or cc-pVTZ leads to the same $ttt < tgt < tg^+g^-$ energy ordering as found by Jaffe et al., although it appears that B3LYP overestimates the *ttt*–*tgt* and *ttt*– tg^+g^- separations. Reoptimization of the geometries at the B3LYP/AVDZ level does not affect these conclusions.

Since it appears to be clear from both refs 26g and 26h, however, that the tg^+g^- conformer **11**—fortuitously found as the lowest energy at the B3LYP/4-21G(*) level—will be the most abundant one in practice, we have used it as the reference structure for the proton affinity calculations.

Protonated glyme ($Gl \cdot H^+$, **12**), on the other hand, is seen to favor a *tgt* rotamer, which permits bonding of the proton to both oxygens, thus forming a five-membered ring. (For a similar small ion, Li^+ , it was previously found^{26h,m} that *tgt* is likewise strongly preferred.) The central proton in **12** is 1.149 and 1.326 Å removed, respectively, from the two oxygens and the methylene groups are almost trans (150°) to the methylene groups. At the B3LYP/4-21G(*) level, this structure is 0.05 kcal/mol lower in energy than the C_2 symmetric structure, where

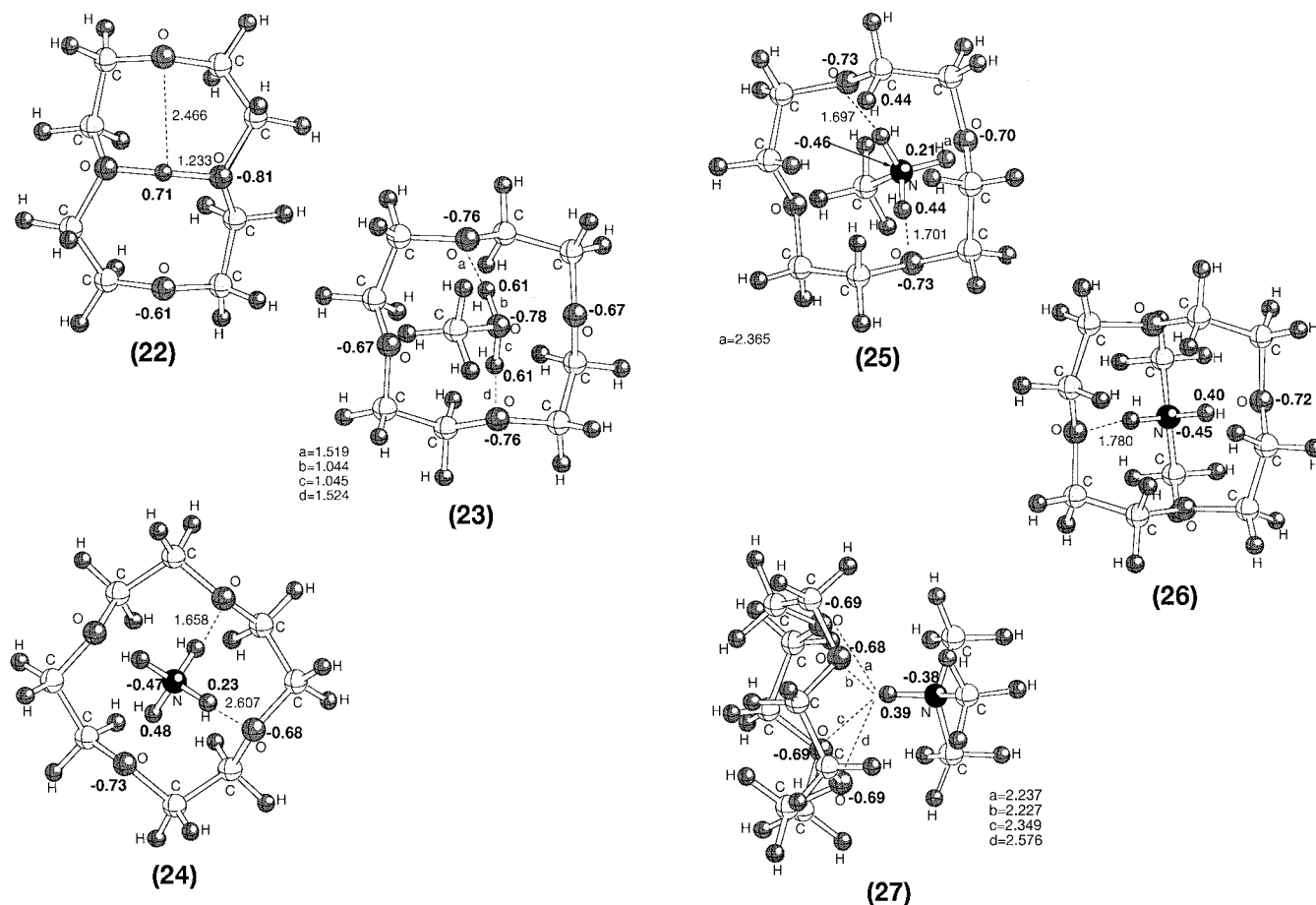


Figure 4. B3LYP/4-21G(*) computed structures of the species 22–27 as well as hydrogen bond distances (Å) and APT atomic charges of some relevant atoms.

the proton would be 1.231 Å away from the oxygens. The small barrier may well be a methodological artifact, and in practice, the effective geometry of the species will probably be symmetric, given such a low barrier. The asymmetry between the two OH distances is however much less pronounced than in the small basis set Hartree–Fock calculations of Meot-Ner et al.²⁸ and Yamabe et al.,²² a similar phenomenon was noted in ref 11. Overall, the structure fairly closely resembles the suggestion in Figure 5 of the experimental work of Vaidyanathan and Garvey.²⁹

In $\text{Gl}\cdot\text{CH}_3\text{OH}_2^+$ (13), although in the initial geometry one of the bridge H atoms is close to glyme, in the optimized geometry both H atoms are close to methanol and 1.463 and 1.436 Å away from the O atoms of glyme. Although the proton affinity of glyme ($\text{PA} = 204.9$ kcal/mol) is higher than that of methanol ($\text{PA} = 181.9$ kcal/mol), it may be that this quasi symmetric geometry is preferred over a nonsymmetric structure that would occur otherwise. Meot-Ner explains the same type of behavior in the complex of H_3O^+ with polyethers where the proton is associated with the H_3O^+ moiety, although the ether groups have higher proton affinities due to the opposing attractions of the ligand groups.²⁸

In $\text{Gl}\cdot\text{NH}_4^+$ (14), NH_3 and glyme have equal proton affinities, but it is NH_3 that attracts the common proton toward itself. The bridges between NH_4^+ and glyme have $\text{O}\cdots\text{H}$ bonds of 1.612 Å and $\text{H}\cdots\text{N}$ bonds of 1.073 Å. The protons of the bridge bear the most positive charge (0.52), and the oxygens of glyme have the most negative charge (−0.77).

$\text{Gl}\cdot\text{NH}_3\text{CH}_3^+$ (15) is quite similar to (14) although not symmetric. Again the bridge protons are the most positive

(0.48) centers and the oxygens are the most negative sites (−0.77). Notice also that $\text{O}\cdots\text{H}$ bonds are longer than in 14 by 0.04 Å.

$\text{Gl}\cdot\text{NH}_2(\text{CH}_3)_2^+$ (16) and $\text{Gl}\cdot\text{NH}(\text{CH}_3)_3^+$ (17) retain the tetrahedral geometry around nitrogen. $\text{Gl}\cdot\text{NH}_2(\text{CH}_3)_2^+$ (16) has two H bonds. Although $\text{Gl}\cdot\text{NH}(\text{CH}_3)_3^+$ (17) is singly hydrogen bonded to one of the glyme oxygens, long-range (2.195 and 2.198 Å) $\text{O}\cdots\text{HC}$ interactions between the other oxygen and two hydrogens from the two nearest methyl groups appear to stabilize this structure. Mautner⁵ has previously reviewed contributions from $-\text{C}-\text{H}^{\delta+}\cdots\text{O}-$ bonds with polyethers. The charge on the bridge H atoms varies from 0.52 in $\text{Gl}\cdot\text{NH}_4^+$ (14) to 0.48 in $\text{Gl}\cdot\text{NH}_3\text{CH}_3^+$ (15) and 0.44 in $\text{Gl}\cdot\text{NH}_2(\text{CH}_3)_2^+$ (16). The charges on the bridge H atoms diminish as the NH_4^+ group changes into $\text{NH}_m(\text{CH}_3)_n^+$ ($m = 1, 3; n = 4 - m$): electron donation from the methyl groups neutralizes the partial positive charge on the bridge proton.

3. Glyme Dimer and Related Complexes. In $(\text{Gl})_2\text{H}^+$ (18), a proton binds one oxygen of one glyme to another oxygen of another glyme, staggered to the first. $\text{O}\cdots\text{H}$ bond lengths are around 1.215 and 1.223 Å. The most negative sites are the oxygens (−0.82) hydrogen bonded to the central proton (0.77). Vaidyanathan and Garvey (Figure 6 in ref 29) suggest the two glymes to be at (almost) right angles, each with one hydrogen bond and one weak ion–dipole interaction. Our computed bond distances, as well as the computed $\text{O}-\text{O}-\text{O}$ dihedral angle of 280° , fundamentally agree with this picture. Contrary to Figure III of Mautner et al.,^{28a} we definitely find the proton to be nearly symmetrically bound to two oxygens rather than predominantly to one. In $(\text{Gl})_2\text{CH}_3\text{OH}_2^+$ (19), the $\text{O}\cdots\text{H}$ bond

lengths are extended to 1.470 and 1.486 Å. In $(\text{Gl})_2\text{NH}_4^+$ (**20**) the $\text{N}\cdots\text{H}$ bond lengths are 1.758 Å. Bond length differences in **19** and **20** may be rationalized in terms of the nature of the electronegative atom in the ligand. In **19** oxygen still has a lone pair capable of assisting the H by donating its electrons and shortening the $\text{H}\cdots\text{O}$ bond, whereas in **20**, N cannot show similar behavior. Structure **20** has four $\text{O}\cdots\text{H}$ bonds because of the symmetric tetrahedral geometry of NH_4^+ and agrees quite well with the previously suggested structure by Feng and Lifshitz⁷ for $(\text{Gl})_2\text{NH}_4^+$ based upon experimental findings only, although some of the other structures suggested intuitively⁷ have to be revised following the present density functional calculations (see coming section).

4. 12-Crown-4 and Related Complexes. It is known³⁰ that the crowns can adapt their conformation for optimum complexation of the guest, a consequence of their dynamic flexibility in solution. There are numerous possible conformations³¹ for the isolated 12-crown-4 molecule (12c4), but in the solid state only a few of these conformations have been observed.³² In the C_4 conformation the four O atoms form a plane with the CH_2 groups on one side. In each $\text{OCH}_2\text{---CH}_2\text{---}$ group one C is closer to the O atom plane ("up" position) and the second C is further from the O atom plane ("down" position). " C_4 " is used to describe the group of structures based on an idealized molecule with true C_4 symmetry. For pseudo- C_4 symmetry if one goes around the macrocyclic chain from one O atom, the first carbon is down and the next up, a chiral conformation which repeats in the next three OCC units.

The RHF and MP2 optimized structures of the 12c4 ligand have S_4 symmetry.^{26b} The OCCO dihedral angle in 12c4 is 70° , 20° larger than the same angle in the $\text{Li}^+(\text{12c4})$ complex. Both the RHF and MP2 optimized structures of 12c4 are in excellent agreement with the crystal structure of 12c4 reported by Growth.³² For 12-crown-4 (**21**), we have found the S_4 symmetric structure to be 13.91 kcal/mol lower in energy than its C_4 counterpart. The bond lengths are O—C 1.480 Å, C—C 1.526 Å, and C—O 1.469 Å.

While 12c4 is quite floppy, 12c4H^+ (**22**) is fixed by an intramolecular hydrogen bond. Structure **22** has C_2 symmetry with the proton 1.233 Å away from two opposite oxygen atoms. This bond is weaker than the one in **18** due to ring strain as shown by Wasada et al.³³

Both in $12\text{c4H}^+\cdot\text{CH}_3\text{OH}$ (**23**) and $12\text{c4H}^+\cdot\text{NH}_3$ (**24**) there are two hydrogen bonds between the two opposite oxygens and the active protons of the ligands. In $12\text{c4H}^+\cdot\text{CH}_3\text{OH}$ (**23**), $\text{CH}_3\text{---OH}_2^+$ is on top of 12c4 with two $\text{O}\cdots\text{H}$ bonds of 1.519 and 1.524 Å, respectively. In **24**, NH_4^+ is equidistant from the two opposite oxygens; $12\text{c4H}^+\cdot\text{NH}_3$ is completely symmetric, with $\text{O}\cdots\text{H}$ bond lengths of 1.658 Å. When the central base is methylamine (**25**) or dimethylamine (**26**), the ligand is pushed away from the ring, the $\text{O}\cdots\text{H}$ distances being {1.697, 1.701 Å} and 1.780 Å, respectively. The lengthening of the $\text{O}\cdots\text{H}$ distance in $12\text{c4}\cdot\text{NH}_m(\text{CH}_3)_n^+$, ($m = 1, 3$; $n = 4 - m$) as n increases is not similar to the situation observed for $\text{Gl}\cdot\text{NH}_m(\text{CH}_3)_n^+$, ($m = 1, 3$; $n = 4 - m$); it may be that the 12c4 ring pushes away the ligand $\text{NH}_m(\text{CH}_3)_3^+$ as n increases and as the ligand becomes crowded. The structure of $12\text{c4H}^+(\text{CH}_3)_3\text{N}$ (**27**) is different from the other clusters of 12c4H^+ with methylamine derivatives: the proton of $(\text{CH}_3)_3\text{NH}$ is at 2.23 Å from two opposite oxygens in 12c4 and the whole structure is stabilized by these long-range interactions.

12c4H^+ (**22**) has the largest negative charge on the hydrogen-bonded oxygens (−0.81), and the central proton is 0.71. In the other clusters of 12c4 the charges for the oxygens bonded

to the active hydrogens and the ones for the bridge hydrogen themselves are distributed as follows: −0.76, +0.61 in **23**; −0.73, +0.48 in **24**; −0.73, +0.44 in **25**; −0.72, +0.40 in **26**; and −0.69, +0.39 in **27**. These findings seem to reflect the fact that the shorter the hydrogen bonds are, the greater is the charge separation.

5. Proton Affinities and Binding Energies. Two experimental PA values exist for Gl. The higher Mautner et al.^{28a} value of 208.9 kcal/mol however reflects a PA scale^{28b} that is biased upward by 4 kcal/mol (see Szulejko and McMahon³⁵ for details). After taking this into account, our B3LYP/AVDZ value of 203.6 kcal/mol and particularly the estimated B3LYP/AVTZ value of 204.7 kcal/mol are in excellent agreement with experiment. Our calculations for 12c4 yield 217.0 kcal/mol at the B3LYP/AVDZ level or an estimated 217.9 kcal/mol at the B3LYP/AVTZ level, somewhat below the lowest experimental value, 219.6 kcal/mol.⁶ Given the extremely low harmonic frequencies involved, we assume that the RRHO treatment in the thermal corrections could lead to a substantial error. The error margin in our calculations is not necessarily small enough to enable us to rule out the higher (221.0 kcal/mol) experimental value of Sharma et al.³⁶

Even after taking into account the 4 kcal/mol downward shift required for the reported Mautner et al.²⁸ value for Gl_2 , this still leaves a gap of 5 kcal/mol, which is unexpectedly large. The Mautner value implies a much larger association energy for $\text{GIH}^+ + \text{Gl} \rightarrow \text{Gl}_2\text{H}^+$, 27.4 kcal/mol, than was previously found by Kebarle and co-workers,³⁶ 22.8 kcal/mol. As argued by Mautner et al.,²⁸ the dimerization energies should be small because internal hydrogen bonds are broken. If we adopt the Kebarle et al. value for the dimerization energy, we obtain 227.2 kcal/mol, compared to 227.5 kcal/mol from ref 36, and not overly different from our own estimated B3LYP/AVTZ value, 225.5 kcal/mol. Again, we suggest that at least part of the remaining discrepancy between theory and experiment would be due to poor RRHO thermal corrections.

As can be seen from Table 2, differences between B3LYP/4-21G(*) and B3LYP/AVDZ energies may be in the 20–30 kcal/mol range. The subsequent discussion will be based exclusively on the B3LYP/AVDZ results, which were seen above to be quite close to experiment at least for the proton affinities. As also seen from Table 2, the computed reaction enthalpies at 298 K for the two dissociation channels of the $12\text{c4H}^+\cdot\text{CH}_3\text{OH}$ complex, 20.0 and 57.9 kcal/mol, agree excellently with the corresponding experimental values⁴ of 19.5 and 58.3 kcal/mol, respectively.

Regarding the dissociation energies of $\text{Gl}\cdot\text{CH}_3\text{OH}_2^+$ (**13**) and of $\text{Gl}\cdot\text{NH}_4^+$ (**14**) to produce CH_3OH_2^+ and NH_4^+ , respectively (Table 2), the trend observed is seen to be based on the $\text{O}\cdots\text{H}$ and $\text{N}\cdots\text{H}$ bond lengths (Figure 1) in the compounds considered: the shorter and the stronger the bond, the more energy is needed to break it. The binding energy for reactions II and IV displays the relative strength of the proton affinities of CH_3OH and NH_3 : more energy is released when NH_3 is inserted into GIH^+ . Considering $\text{Gl}\cdot\text{NH}_3\text{CH}_3^+$ (**15**), $\text{Gl}\cdot\text{NH}_2(\text{CH}_3)_2^+$ (**16**), and $\text{Gl}\cdot\text{NH}(\text{CH}_3)_3^+$ (**17**) in reactions VII, IX, and XI, it is possible to state that dissociation energies decrease as the number of methyl groups increases. In reaction XI, for $\text{Gl}\cdot\text{NH}(\text{CH}_3)_3^+$ (**17**) the binding energy is considerably smaller than for **14**, **15**, and **16** due to the fact that a single $\text{O}\cdots\text{H}$ bond is broken in **17** whereas two $\text{O}\cdots\text{H}$ bonds are broken in the others. For reactions VI and VIII insertion of methylamine derivatives is expected to be easier as the proton affinity of the ligand increases. As expected, the energy released in these reactions

increases as the number of methyl groups increases in methylamines. Reaction X does not follow this trend because of the single O \cdots H bond as described previously.

Regarding the binding energies of **19** and **20** in reactions XV and XVII (Table 2), the first one refers to the breakage of two H bonds, whereas the second one refers to the cleavage of four H bonds. Binding energies per O \cdots H and N \cdots H bonds amount to 30.8 and 27.7 kcal/mol, respectively; this is in agreement with the expectations based on the shorter H bonds in **19** relative to **20**. Insertion of NH₃ into (Gl)₂H⁺ is more exothermic than insertion of CH₃OH (reactions XVI and XIV).

The binding energies deduced from reactions XIX and XXI show a trend similar to reactions II and IV with almost the same difference of 13 kcal/mol, with ammonia insertion being more exothermic than methanol. For 12c4.NH_m(CH₃)_n⁺, (*m* = 1, 3; *n* = 4 - *m*) the binding energy decreases as the number of methyl groups in the ligand increases as mentioned earlier for (Gl)₂NH_m(CH₃)_n⁺, (*m* = 1, 3; *n* = 4 - *m*). Comparison of the binding energies deduced for reactions XIV and XIX reflects the stability of 12c4H⁺·CH₃OH with respect to (Gl)₂CH₃OH₂⁺; the same is true for reactions XVI and XXI despite the larger number of H bonds in **20** than in **24**. There are four O \cdots H bonds in **20** and only two O \cdots H bonds in **24**, and the ratio of the binding energies per hydrogen bond for reactions XVI and XXI is larger than that for reactions XIV and XIX, where the number of O \cdots H bonds is the same. It can be concluded that ammonia/methanol insertion into 12c4H⁺ relative to (Gl)₂H⁺ is more exothermic per hydrogen bond for the former than for the latter. These findings are in agreement with the experimental observations of Feng and Lifshitz,⁷ where ammonia insertion into 12c4H⁺ was found to be 1 order of magnitude more efficient than its insertion into (Gl)₂H⁺; the same protonated species were found to be equally efficient toward methanol.

Experimental work on protonated complexes containing ligands with a total of four polar groups has shown increasing binding energies with increasing flexibility of the ligands,²⁶ and this behavior was attributed to the stabilization of the proton by the free ether groups. The same is true for reactions XVIII and XII, where the calculated binding energy for (Gl)₂H⁺ is higher than the one for 12c4H⁺.

Agreement between computed RRHO entropies and available experimental values is quite poor due to the limitations inherent in RRHO theory for the present systems, and we have not pursued this point further.

IV. Conclusions

We draw a number of conclusions from this study.

The geometric features of the optimized clusters with B3LYP/4-21G(*) agree with experimental findings (where available) and with a priori expectations.

The B3LYP/avg-cc-pVDZ//B3LYP/4-21G(*) level of theory is found to be a particularly good compromise between CPU time and quality of results for proton affinities (and related reaction energies) of medium-sized molecules. Reaction enthalpies for the protonated clusters at this level of theory are in very good agreement with experimental data where the latter are available. The "diffuse" part of the avg-cc-pVDZ basis set is found to be more essential than extension of the underlying basis set from cc-pVDZ to cc-pVTZ. The great improvement in agreement between B3LYP and experimental proton affinities upon adding diffuse functions to the basis set is directly related to a drastic reduction in the counterpoise-estimated basis set superposition error.

Insertion of NH₃ into GlH⁺, (Gl)₂H⁺ and 12c4H⁺ is more exothermic than insertion of CH₃OH into the same protonated species.

Dissociation energies to produce the protonated bases reflect the strength of the O \cdots H bonds: more energy is required to break O \cdots H bonds when the base is methanol rather than ammonia and methylamine(s).

Insertion of NH₃ into 12c4H⁺ is more exothermic than its insertion into (Gl)₂H⁺; the exothermicity for the insertion of CH₃OH is comparable for 12c4H⁺ and (Gl)₂H⁺.

Acknowledgment. D.A. and V.A. acknowledge the support from the Bogaziçi University Research Funds. J.M. is a Yigal Allon Fellow and an Honorary Research Associate ("Onderzoeksleider in Eremandaat") of the National Science Foundation of Belgium. The authors thank Mr. Olivier Uzan and Mrs. Miriam Ahituv for their assistance with the figures and Drs. David Feller and Richard L. Jaffe for critical reading of the manuscript prior to publication. This research was supported by The Israel Science Foundation founded by the Israel Academy of Sciences and Humanities. The Farkas Research Center is supported by the Minerva Gesellschaft für die Forschung GmbH, München.

Supporting Information Available: Table of total energies and zero-point energies (1 page). Ordering information is given on any current masthead page.

References and Notes

- (1) Pedersen, C. J. *J. Am. Chem. Soc.* **1967**, *89*, 7017.
- (2) (a) Lehn, J. M. *Acc. Chem. Res.* **1978**, *11*, 49. (b) More, M. B.; Ray, D.; Armentrout, P. B.; *J. Phys. Chem. A* **1997**, *101*, 831, 4254, 7007.
- (3) Meot-Ner (Mautner), M. *J. Am. Chem. Soc.* **1983**, *105*, 4912.
- (4) Sharma, R. B.; Kebarle, P. J. *Am. Chem. Soc.* **1984**, *106*, 3913.
- (5) Meot-Ner (Mautner), M. *Acc. Chem. Res.* **1984**, *17*, 186.
- (6) Meot-Ner (Mautner), M. *J. Am. Chem. Soc.* **1983**, *105*, 4906.
- (7) Feng, W. Y.; Lifshitz, C. J. *Am. Chem. Soc.* **1995**, *117*, 11548.
- (8) Feng, W. Y.; Goldenberg, M.; Lifshitz, C. *J. Am. Chem. Soc. Spectrom.* **1994**, *5*, 695.
- (9) Feng, W. Y.; Lifshitz, C. *Int. J. Mass. Spectrom. Ion Processes* **1995**, *149/150*, 13.
- (10) Feng, W. Y.; Ling, Y.; Lifshitz, C. *J. Phys. Chem.* **1996**, *100*, 35.
- (11) Martin, J. M. L.; Aviyente, V.; Lifshitz, C. *J. Phys. Chem.* **1997**, *101*, 2597.
- (12) Frisch, M. J.; Trucks, G. W.; Schlegel, H. B.; Gill, P. M. W.; Johnson, B. G.; Robb, M. A.; Cheesman, J. R.; Keith, T.; Petersson, G. A.; Montgomery, J. A.; Raghavachari, K.; Al-Laham, M. A.; Zakrzewski, V. G.; Ortiz, J. V.; Foresman, J. B.; Cioslowski, J.; Stefanov, B. B.; Nanayakkara, A.; Challacombe, M.; Peng, C. Y.; Ayala, P. Y.; Chen, W.; Wong, M. W.; Andres, J. L.; Replogle, E. S.; Gomperts, R.; Martin, R. L.; Fox, D. J.; Binkley, J. S.; Defrees, D. J.; Baker, J.; Stewart, J. J. P.; Head-Gordon, M.; Gonzales, C.; Pople, J. A. *GAUSSIAN 94*, Revision C.2; Gaussian Inc.: Pittsburgh, PA, 1995.
- (13) Stewart, J. J. P. *J. Comput. Chem.* **1989**, *10*, 209, 221.
- (14) SPARTAN version 4.0; Wavefunction, Inc.: 18401 Von Karman Ave., #370 Irvine, CA 92715.
- (15) Becke, A. D. *J. Chem. Phys.* **1993**, *98*, 5648.
- (16) Lee, C.; Yang, W.; Parr, R. G. *Phys. Rev.* **1988**, *B37*, 785.
- (17) (a) Devlin, F. J.; Finley, J. W.; Stephens, P. J.; Frisch, M. J. *J. Phys. Chem.* **1995**, *99*, 16883. (b) Martin, J. M. L.; El-Yazal, J.; François, J. P. *Mol. Phys.* **1995**, *86*, 1437. (c) Rauhut, G.; Pulay, P. *J. Phys. Chem.* **1995**, *99*, 3093. (d) Wong, M. W. *Chem. Phys. Lett.* **1996**, *256*, 391.
- (18) Pulay, P.; Fogarasi, G.; Pang, F.; Boggs, J. E. *J. Am. Chem. Soc.* **1979**, *101*, 2550.
- (19) Pang, F.; Pulay, P.; Boggs, J. E. *J. Mol. Struct. (THEOCHEM)* **1982**, *88*, 79. See also: Martin, J. M. L.; François, J. P.; Gijbels, R. J. *Comput. Chem.* **1989**, *10*, 346, for an application to proton affinities.
- (20) (a) Dunning, T. H., Jr. *J. Chem. Phys.* **1989**, *90*, 1007. (b) Kendall, R. A.; Dunning, T. H., Jr.; Harrison, R. J. *J. Chem. Phys.* **1992**, *96*, 6796.
- (21) Martin, J. M. L.; Lee, T. J. *J. Chem. Phys. Lett.* **1996**, *258*, 136.
- (22) Yamabe, S.; Hirao, K.; Wasada, H. *J. Phys. Chem.* **1992**, *96*, 10261.
- (23) (a) Boys, S. F.; Bernardi, F. *Mol. Phys.* **1970**, *19*, 553, 22. (b) Halkier, A.; Koch, H.; Jørgensen, P.; Christiansen, O.; Beck Nielsen, I. M.; Helgaker, T. *Theor. Chem. Acc.* **1997**, *97*, 150. (c) Martin, J. M. L.; Lee, T. J.; Taylor, P. R. *J. Chem. Phys.* **1998**, *108*, 676.

(24) (a) Cioslowski, J. *J. Am. Chem. Soc.* **1989**, *111*, 8333. (b) Martin, J. M. L.; Van Alsenoy, C. *GAR2PED*; University of Antwerp, 1995. (c) De Proft, F.; Martin, J. M. L.; Geerlings, P. *Chem. Phys. Lett.* **1996**, *250*, 393.

(25) (a) Andersson, M.; Karlström, G. *J. Phys. Chem.* **1990**, *94*, 4299. (b) Abe, A.; Tasaki, K. *J. Mol. Struct.* **1986**, *145*, 309. (c) Barzaghi, M.; Gamba A.; Morosi, G., *J. Mol. Struct.* **1988**, *170*, 69. (d) Bressanini, D.; Gamba A.; Morosi, G. *J. Phys. Chem.* **1990**, *94*, 4299.

(26) (a) Matsuura H.; Miyazawa T., Machida K. *Spectrochim. Acta* **1973**, *29A*, 771. (b) Miyake A. *J. Am. Chem. Soc.* **1960**, *82*, 3040. (c) Machida, K.; Miyazawa T. *Spectrochim. Acta* **1964**, *20*, 1865. (d) Iwamoto R. *Spectrochim. Acta* **1971**, *27A*, 2385. (e) Ogawa, Y.; Ohta, M.; Sakakibara, M.; Matsuura H.; Harada, I.; Shimanouchi, T. *Bull. Chem. Soc. Jpn.* **1977**, *50*, 650. (f) Astrup, E. E. *Acta Chem. Scand.* **1979**, *A33*, 655. (g) Jaffe, R. L.; Smith, G. D.; Yoon, D. Y. *J. Phys. Chem.* **1993**, *97*, 12745. (h) Ray, D.; Feller, D.; More, M. B.; Glendening, E. D.; Armentrout, P. B. *J. Phys. Chem.* **1996**, *100*, 16116. (i) Murcko, M. A.; DiPaola, R. A. *J. Am. Chem. Soc.* **1992**, *114*, 10010. (j) Reiling, S.; Brickmann, J.; Schlenkrich, M.; Bopp, P. A. *J. Comput. Chem.* **1996**, *17*, 133. (k) Feller, D. *J. Chem. Phys.* **1992**, *96*, 6104. (l) Yoshida, H.; Tanaka, T.; Matsuura, H. *Chem. Lett.* **1996**, *8*, 637. See also Yoshida, H.; Kaneko, I.; Matsuura, H.; Ogawa, Y.; Tasumi,

M. *Chem. Phys. Lett.* **1992**, *196*, 601. (m) Smith, G. D.; Jaffe, R. L.; Partridge, H. *J. Phys. Chem. A* **1997**, *101*, 1705.

(27) Inomata, K.; Abe, A. *J. Phys. Chem.* **1992**, *96*, 7934.

(28) (a) Meot-Ner, M.; Sieck, L. W.; Scheiner, S.; Duan, X. *J. Am. Chem. Soc.* **1994**, *116*, 7848. (b) Mautner (Meot-Ner), M.; Sieck, L. W. *J. Am. Chem. Soc.* **1991**, *113*, 4448.

(29) Vaidyanathan, G.; Garvey, J. F. *J. Phys. Chem.* **1994**, *98*, 2248.

(30) Ratcliffe, C. I.; Buchanan, G. W.; Denike, J. K. *J. Am. Chem. Soc.* **1995**, *117*, 2900.

(31) Seidl, E. T.; Schaefer, H. F., III. *J. Phys. Chem.* **1991**, *95*, 3589.

(32) Growth, P. *Acta Chem. Scand. Ser. A* **1981**, *35*, 463.

(33) Wasada, H.; Tsutsui, Y.; Yamabe, S. *J. Phys. Chem.* **1996**, *100*, 7367.

(34) Meot-Ner, M.; Sieck, L. W.; Liebman, J. F.; Scheiner, S. *J. Phys. Chem.* **1996**, *100*, 6445.

(35) Szulejko, J. E.; McMahan, T. B. *J. Am. Chem. Soc.* **1993**, *115*, 7839.

(36) Sharma, R. B.; Blades, A. T.; Kebarle, P. J. *J. Am. Chem. Soc.* **1984**, *106*, 510.

(37) Lias, S. G.; Liebman, J. F.; Levin, R. D. *J. Phys. Chem. Ref. Data* **1984**, *13*, 695.